ULTRAPETALA1 encodes a SAND domain putative transcriptional regulator that controls shoot and floral meristem activity in *Arabidopsis*

Cristel C. Carles[1,2], Dan Choffnes-Inada[1,2], Keira Reville[1,2,*], Kvin Lertpiriyapong[2] and Jennifer C. Fletcher[1,2,†]

[1]Plant Gene Expression Center, USDA/UC Berkeley, 800 Buchanan Street, Albany, CA 94710 USA
[2]Plant and Microbial Biology Department, UC Berkeley, 111 Koshland Hall, Berkeley, CA 94720 USA
*Present address: Department of Medicine and Therapeutics, Conway Institute of Biomolecular and Biomedical Research, University College Dublin, Dublin 4, Ireland
†Author for correspondence (e-mail: fletcher@nature.berkeley.edu)

Development 132, 897-911
Published by The Company of Biologists 2005
doi:10.1242/dev.01642

Accepted 14 December 2004

Summary

The higher-plant shoot apical meristem is a dynamic structure continuously producing cells that become incorporated into new leaves, stems and flowers. The maintenance of a constant flow of cells through the meristem depends on coordination of two antagonistic processes: self-renewal of the stem cell population and initiation of the lateral organs. This coordination is stringently controlled by gene networks that contain both positive and negative components. We have previously defined the *ULTRAPETALA1* (*ULT1*) gene as a key negative regulator of cell accumulation in *Arabidopsis* shoot and floral meristems, because mutations in *ULT1* cause the enlargement of inflorescence and floral meristems, the production of supernumerary flowers and floral organs, and a delay in floral meristem termination. Here, we show that *ULT1* negatively regulates the size of the *WUSCHEL* (*WUS*)-expressing organizing center in inflorescence meristems. We have cloned the *ULT1* gene and find that it encodes a small protein containing a B-box-like motif and a SAND domain, a DNA-binding motif previously reported only in animal transcription factors. ULT1 and its *Arabidopsis* paralog ULT2 define a novel small gene family in plants. *ULT1* and *ULT2* are expressed coordinately in embryonic shoot apical meristems, in inflorescence and floral meristems, and in developing stamens, carpels and ovules. Additionally, *ULT1* is expressed in vegetative meristems and leaf primordia. ULT2 protein can compensate for mutant ULT1 protein when overexpressed in an *ult1* background, indicating that the two genes may regulate a common set of targets during plant development. Downregulation of both ULT genes can lead to shoot apical meristem arrest shortly after germination, revealing a requirement for ULT activity in early development.

Key words: *Arabidopsis thaliana,* ULTRAPETALA, Shoot apical meristem, SAND domain, B box domain

Introduction

Meristems, as centers of cell proliferation and organ initiation, are the foundation of all plant structures. After germination, the shoot apical meristem (SAM) and the root apical meristem (RAM) grow in opposite directions to generate the aerial and underground parts of the plant. The cells produced by the SAM develop into stem tissue, leaves and flowers, and also form axillary meristems that reiterate the development of the primary SAM. The constant formation of new organs and tissues throughout plant life relies on precise mechanisms that maintain overall meristem integrity for upwards of hundreds of years in some species.

The SAM persists as a cell dome with both a longitudinal and a radial structure (Steeves and Sussex, 1989). In most dicots, the SAM is divided into three clonally distinct layers. Cells in the outermost layer (L1) produce epidermal tissues, whereas cells of the sub-epidermal layer (L2) and the internal layers (L3) differentiate into vascular and internal tissues. Superimposed across these cell layers are distinct zones of differential meristem activity. A central zone (CZ) at the very apex harbors the unspecialized stem cells, which maintain themselves and also replenish cells in the adjacent peripheral zone (PZ) as they are lost during the formation of lateral organ primordia on the meristem flanks. Maintenance of SAM integrity requires a precise coordination between the flow of cells leaving the PZ and their replacement by cells from the CZ, which implies that the different regions of the meristem are in communication with one another. In *Arabidopsis*, one key component of the meristem communication system is the CLAVATA (CLV) extracellular signaling pathway.

In *clavata* mutants (*clv1*, *clv2*, *clv3*), all aerial meristems produce a greatly increased cell population, resulting in the formation of fasciated stems, supernumerary flowers and flowers with extra organs (Clark et al., 1993; Clark et al., 1995; Kayes and Clark, 1998). At the other extreme, *wuschel* (*wus*) mutants undergo premature termination of their shoot and floral meristems (Laux et al., 1996). *WUS,* which encodes a homeodomain transcription factor (Mayer et al., 1998), is expressed in a small region in the meristem interior referred to as the organizing center (OC), from where it specifies stem cell

identity on the overlying L1 and L2 cells (Schoof et al., 2000). The stem cell-promoting activity of WUS is counterbalanced by the CLV proteins, which are members of a signal transduction pathway that limits the size of the *WUS*-expressing cell population (Clark et al., 1997; Fletcher et al., 1999; Jeong et al., 1999; Trotochaud et al., 1999). In *clv* mutant meristems, the *WUS* expression domain expands laterally and upwards, leading to the accumulation of excess stem cells (Brand et al., 2000; Schoof et al., 2000). Thus, the activity of the CLV pathway establishes a negative feedback loop between the stem cells and the underlying organizing center that maintains meristem homeostasis throughout development (Brand et al., 2000; Gallois et al., 2002; Lenhard and Laux, 2003; Schoof et al., 2000).

Maintenance of a functional SAM also requires additional factors that act in pathways independent of the CLV pathway. For example, a number of *Arabidopsis* mutants that are impaired in chromatin assembly or genome maintenance display pleiotropic phenotypes, including severely disorganized cell arrangements at both the shoot and root apices. Among these are *fasciata1* (*fas1*) and *fas2* (Leyser and Furner, 1992), *mre11* (Bundock and Hooykaas, 2002), the *AtCAP-E1* and *AtCAP-E2* condensin mutants (Siddiqui et al., 2003), and *tonsoku/mgoun3/bru1* (Guyomarc'h et al., 2004; Suzuki et al., 2004; Takeda et al., 2004). Likewise, mutations in the *HALTED ROOT* (*HLR*) gene, which encodes a subunit of the 26S proteasome, result in the disorganization of the SAM and the RAM that correlates with a disturbed shoot organizing center and root quiescent center (Ueda et al., 2004). For most of these mutants, the observed stem fasciation phenotypes are linked to the distortion of the *WUS* expression pattern in the SAM in a broader and more random manner than occurs in the *clv* mutants. Mutations in the farnesyltransferase gene *ENHANCED RESPONSE TO ABSCISIC ACID1* (Running et al., 1998; Ziegelhoffer et al., 2000) and the prenyltransferase gene *PLURIPETALA* (Running et al., 2004) also increase SAM size in a CLV-independent manner.

We have previously identified ULTRAPETALA1 (ULT1) as an additional factor that negatively regulates *Arabidopsis* shoot and floral meristem activity, as *ult1* mutations cause the enlargement of inflorescence and floral meristems, leading to the production of supernumerary flowers and floral organs (Fletcher, 2001). *ult1* mutants also have reduced floral meristem determinacy, and ULT1 has been shown to negatively regulate *WUS* expression in order for floral meristem termination to occur at the correct stage of flower development (Carles et al., 2004). Here, we report the cloning and characterization of the *ULT1* gene and its paralog *ULT2*. We show that the organization of the SAM is not altered in *ult1* mutants, but that ULT1 restricts the size of the *WUS*-expressing cell population. *ULT1* and *ULT2* encode small proteins containing a SAND DNA-binding motif and a B box-like domain, and their expression patterns fully overlap in inflorescence meristems, floral meristems and reproductive organs. Both genes are also expressed in embryos, but only *ULT1* mRNA accumulates in vegetative meristems and leaf primordia. We discuss the functions of the ULT factors throughout plant development, and in light of what is known about SAND domain-containing factors in animals, we propose that the ULT proteins may act as direct regulators of developmental gene expression.

Materials and methods

Plant material and growth conditions

Landsberg *erecta* (L*er*), the ecotype in which the *ult1* ethyl methanesulfonate (EMS) alleles were isolated, was used as the wild-type strain for the *ult1* alleles. The STM promoter-GUS line (L*er* ecotype) was obtained from Anita Fernandez and Kathy Barton. The *ult1-3* allele (SALK 074642) and *ult2-1* allele (SAIL 748C4) were initially isolated from T-DNA mutagenesis populations in the Columbia-0 (Col-0) background. The *ult1-3* allele was introgressed into L*er* through three backcrosses. Plants were grown in a 1:1:1 mixture of perlite:vermiculite:topsoil under continuous cool-white fluorescent lights (120 μmol m^{-2} s^{-1}) at 22°C, and were watered daily with a 1:1500 dilution of Miracle-Gro 20-20-20 fertilizer. Transgenic lines were generated by the floral dip method (Clough and Bent, 1998).

Mapping and molecular identification of *ULT1*

Using cleaved amplified polymorphic sequence (CAPS) markers (Konieczny and Ausubel, 1993) distributed across the lower arm of chromosome 4, we established that *ult1-2* was flanked by markers PG11 (map position 75.16 cM) and g8300 (81.22 cM). For the fine mapping of *ULT1*, we designed 12 new CAPS markers that spanned the region between markers PG11 and g8300, using the TIGR Landsberg *erecta* random sequence database (www.tigr.org) as a source for single nucleotide polymorphisms (SNPs). The primer sequences, restriction enzyme and number of restriction sites in the Col/L*er* ecotypes for the CAPS marker sequences generated across this interval are available upon request.

Sequencing was performed on an ABI PRISM® 3100 Genetic Analyzer sequencer (Perkin Elmer), according to the manufacturer's instructions. Computer-based sequence analysis was performed using VectorNTI® Suite (Informax) and Sequencher (Gene Codes Corporation, Ann Harbor) software. Multiple protein alignments were obtained using ClustalX and edited with SeqVu (The Garvan Institute of Medical Research).

Construction of transgenic lines

ULT1-214 complementation construct

A 2745 bp fragment spanning the *ULT1*-coding region and flanking sequence was digested from BAC F26K10 with *Nde*I, Klenow-filled and cloned into blunt pBSK+ vector (pBSK$^+$-ULT construct). Then a *Bam*HI/*Kpn*I fragment was cut from pBSK$^+$-ULT vector and cloned into the binary vector pCD214 (kindly provided by Chris Day). Transgenic plants were selected on MS plates containing gentamycin (100 μg/ml).

d35S::ULT1/d35S::ULT2 sense and d35S::ULT1 antisense constructs

The full-length ULT ORFs were cloned into the binary vector pCD223 (kindly provided by Chris Day) at the *Eco*RI site, flanked 5′ by a double CaMV 35S promoter and 3′ by a nopaline synthase transcription termination signal. The clones were then screened by PCR to obtain the ULT cDNA insert in the sense (S) or antisense (AS) orientation. Transgenic plants were selected on MS plates containing gentamycin (100 μg/ml).

35S::ULT-$(Ala)_{10}$-GFP and 35S:: ULT-$(Ala)_{10}$-GUS-GFP constructs

The pEZS vectors carrying the CaMV 35S-MCS-$(Ala)_{10}$-EGFP cassette or the CaMV 35S-EGFP-$(Ala)_{10}$-MCS cassette were kindly provided by David Ehrhardt. The ULT cDNA fragments were cloned into the *Eco*RI and *Bam*HI sites of pEZS-NL/CL vectors to give pEZS-NL/CL-ULT constructs. To create the CaMV 35S-MCS-$(Ala)_{10}$-GUS-EGFP and CaMV 35S-GUS-EGFP-$(Ala)_{10}$-MCS cassettes, we introduced a short synthetic linker at the *Nco*I site of pEZS. The β-Glucuronidase *uidA* (*GUS*) gene was cloned at the newly created *Nco*I and *Pml*I sites. Then the ULT cDNA fragments were

cloned into the *Eco*RI and *Bam*HI sites of the pEZS MCS. For stable transformation of *Arabidopsis* plants, the 35S::ULT-GFP and 35S::ULT-GUS-GFP cassettes were transferred into pART27 at the *Not*I site (Gleave, 1992). Transgenic plants were then selected on MS plates containing kanamycin (50 μg/ml).

Subcellular localization

For transient assays, the pEZS-ULT fusions were transformed into onion epidermis cells by particle bombardment using a Biolistic PDS-1000/He unit (BioRad, Richmond, CA), as described (Sanford et al., 1993). For GFP visualization, epidermal peels were examined 24-36 hours after bombardment using a Zeiss Axiophot microscope. GFP fluorescence was visualized with the FITC channel and images were acquired with a 12-bit MicroMax cooled CCD camera operated by IPLab software (Scanalytics, Fairfax, VA). GFP and DAPI fluorescence was visualized in plants using a Zeiss LSM510 confocal laser-scanning microscope (CLSM), with the FITC channel and the UV channel, respectively.

For immunodetection of GFP in the transgenic lines, 0.5 g of inflorescence tissues were ground in liquid nitrogen and then extracted with 500 μl of cold buffer [100 mM MOPS pH 7.6, 100 mM NaCl, 5% (v/v) Glycerol, 1 mM EDTA, 14 mM β-mercaptoethanol, 1 mM PMSF, 2 μg/ml pepstatin A, 0.2 μg/ml leupeptin, 1 μg/ml aprotinin] containing protease inhibitors. Each protein extract (15 μg) was separated on a 12.5% SDS-PAGE gel and blotted on a nitrocellulose membrane. Immunoblots were incubated with a 1:500 dilution of an anti-GFP polyclonal antibody (Santa Cruz Biotech).

GUS staining

The GUS staining reaction and subsequent tissue embedding and sectioning were performed as described (Sieburth and Meyerowitz, 1997), with the exception that GUS localization was visualized after 6 hours of staining with 2 mM of 5-bromo-4-chloro-3-indolyl-β-D-glucoronide (X-GLUC, Bioworld).

RT-PCR

Total RNA was isolated from various tissues using the RNeasy plant kit (Qiagen), treated with RQ1 RNase-free DNase (Promega) for 30 minutes at 37°C, and then purified with phenol/chloroform. The first-strand cDNA synthesis was performed on 5 μg of total RNA using Superscript II RNase H^- reverse transcriptase (Gibco BRL, Life Technologies) and an oligo dT primer (18 mer), according to the manufacturer's instructions. From 20 μl of the reverse-transcription (RT) product, 1 μl was used for each PCR reaction. The annealing temperature was 54°C for all primer pairs and 34 cycles of PCR were performed for all genes, except when mentioned otherwise.

In situ hybridization

Probes for in situ hybridization were transcribed using the digoxigenin-labeling mix (Roche). The *WUS* antisense probe was generated as described previously (Mayer et al., 1998). The *STM* antisense probe was generated from the 1.1 kb transcript described by Long and Barton (Long and Barton, 1998). Separate ULT probes were generated from the full-length coding sequences of *ULT1*and *ULT2,* and from the 3′UTR of each gene. Tissue fixation and in situ hybridization were performed as described previously (Ambrose et al., 2000), with the additional steps that siliques were smashed and seedlings tips were chopped before infiltration, to facilitate fixative penetration into the tissues.

Results

ULTRAPETALA1 negatively regulates the size of the *WUS*-expressing organizing center during reproductive development

Previous analysis of the EMS-induced *ult1-1* and *ult1-2* alleles revealed an increase in inflorescence and floral meristem size, leading to the production of supernumerary flowers and floral organs (Fletcher, 2001) (Fig. 1A-C). To determine the molecular basis of the *ult1* meristem enlargement, we performed in situ experiments to analyze the expression pattern of *STM* as a marker for inflorescence meristem fate. *STM* is expressed throughout wild-type inflorescence and floral meristems (Long and Barton, 2000; Long et al., 1996), and is absent from the flanking region that corresponds to the incipient flower and floral organ primordia (Fig. 1E). We did not detect any major changes in the overall pattern of *STM* expression in *ult1-1* and *ult1-2* inflorescence meristems. *STM* expression is visible in the central part of the inflorescence and floral meristems and absent from the peripheral region. However, the domain expressing *STM* is more extensive in *ult1* mutant meristems than in wild-type meristems (Fig. 1E-G). This result shows that the supernumerary cells present in *ult1* mutant meristems (Fletcher, 2001) correspond to meristem cells rather than to lateral organ primordia cells.

To determine whether the *ult1* meristem enlargement occurs uniformly across the shoot apex or is confined to one area, we examined the expression patterns of molecular markers for specific meristematic regions in *ult1* inflorescences. We have previously reported that the *CLV1* expression domain, which corresponds to the most central L3 cells of the SAM, is significantly broader in *ult1-1* inflorescence meristems than in wild type (Fletcher, 2001). This result suggested a function for ULT1 in restricting cell accumulation in the interior, central region of the meristem. By contrast, the *CLV3* expression pattern in the L1 and L2 layers of the central zone appeared to be unchanged in *ult1-1* meristems (Fletcher, 2001), either because the *CLV3* expression domain is not affected by the mutation, or because its enlargement across such a small group of cells is too slight to be noticed by in situ hybridization.

The *WUS* gene is expressed in the interior, deeper layers of shoot and floral meristems, overlapping the *CLV1* expression domain (Fig. 1I) (Mayer et al., 1998). Mutations in *ULT1* result in the lateral expansion of the *WUS* expression domain, without altering its layer specificity (Fig. 1J-K). Counting of *WUS*-expressing cells confirmed that the organizing center is significantly larger in *ult1-1* and *ult1-2* meristems than in wild-type meristems (Fig. 1P). In wild-type inflorescence meristems, the mean size of the *WUS*-expressing domain corresponds to 6.12±0.33 cells in width, 3±0 cells in height and 14.75±0.97 cells in total. In *ult1-1* inflorescence central sections the *WUS* domain expands to 8.50±1 cells in width, 3.12±0.33 cells in height, and 21.12±2.80 cells in total, while in *ult1-2* inflorescence central sections the *WUS* domain is 7.75±0.66 cells in width, 3±0 cells in height and 18±1.66 cells in total. This result shows that the size of the *WUS*-expressing organizing center is negatively regulated by ULT1 activity. As *ult1-1* plants have larger inflorescence and floral meristems than do *ult1-2* plants and produce more floral meristems and floral organs (Fletcher, 2001), our results suggest that the size of the *WUS*-expressing organizing center may directly affect these traits.

Finally, we used a p*STM::uidA* (McConnell and Barton, 1998) reporter line as a marker to examine the size of the peripheral zone of the meristem in wild-type and *ult1* plants. This reporter construct does not recapitulate the *STM* expression pattern in the meristem; instead, it is expressed at

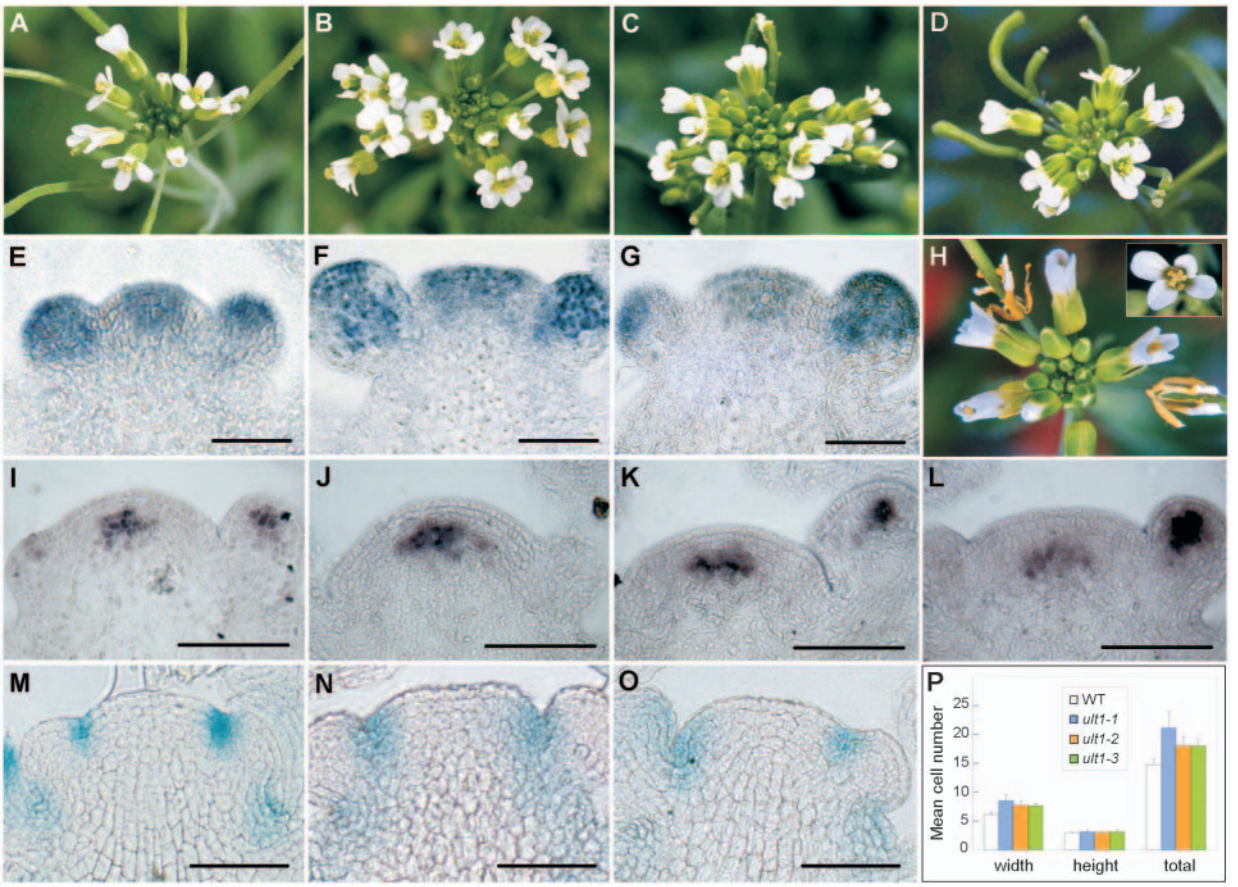

Fig. 1. Inflorescence and flower phenotypes of *ult1* mutants and complementation test. (A-D) Inflorescence meristems of (A) wild-type L*er,* (B) *ult1-1*, (C) *ult1-2* and (D) *ult1-3* plants. (E-G) In situ expression analysis of *STM* in (E) L*er*, (F) *ult1-1* and (G) *ult1-2* inflorescences. (H) Inflorescence and (inset) flower of *ult1-1* plants transformed with the ULT1-214 construct containing a 2.7 kb *ULT1* genomic fragment. (I-L) In situ expression analysis of *WUS* in (I) L*er*, (J) *ult1-1*, (K) *ult1-2* and (L) *ult1-3* inflorescences. (M-O) Analysis of p*STM::uidA* expression in (M) L*er*, (N) *ult1-1* and (O) *ult1-2* inflorescences. (P) Quantification of *WUS*-expressing cells in L*er* (WT) and all three *ult1* alleles. The mean number of cells was calculated from the most central section of eight individual inflorescences for each genotype. For each section, the maximum number of cells found in one horizontal (width) and one vertical (height) cell file, as well as the total number of cells expressing *WUS*, was scored. The standard deviation is indicated. Scale bars: 50 μm.

the boundary between the proper inflorescence meristem and the incipient floral primordia (Fig. 1M). The p*STM::uidA* expression pattern is unaltered in *ult1* inflorescences, indicating that the peripheral region of the mutant meristems is not significantly enlarged (Fig. 1N-O). Altogether, our expression analyses indicate that ULT1 restricts the lateral expansion of *CLV1*- and *WUS*-expressing cells in the interior of inflorescence and floral meristems.

Positional cloning of *ULT1*

To isolate the *ULT1* gene, we used CAPS-based mapping (Konieczny and Ausubel, 1993) of recombination breakpoints in 1366 meiotic events among the F2 progeny of *ult1-2* (L*er*) × wild type (Col-O). We had previously shown that the *ult1* mutations mapped between the visible markers *ag* and *ap2* on chromosome 4 (Fletcher, 2001). Using the CAPS markers throughout this interval, we established that *ult1-2* was flanked by markers PG11 and g8300 (www.arabidopsis.org). Thirty-one plants with recombination events between PG11 and g8300 were identified from the mapping population, and used to refine the position of the *ult1-2* recombination breakpoints to the ends of BAC F26K10. We sequenced candidate genes annotated on the BAC and identified a single gene (At4g28190) that was mutated in both *ult1* alleles.

To confirm the identity of At4g28190 as the *ULT1* gene, a genomic clone (ULT1-214) containing the At4g28190 coding region along with 1 kb of upstream and 0.5 kb of downstream sequence was introduced into *ult1-1* plants, and this clone partially or fully complemented the mutant phenotypes (Fig. 1H). T1 and T2 *ult1-1* plants transformed with the ULT1-214 genomic construct produced meristems and flowers similar to those of wild-type plants. In addition, *ult1-1* plants carrying the ULT1-214 transgene flowered at the same time as did wild-type plants, while untransformed *ult1-1* plants flowered 1 week later on average (Fletcher, 2001). These data confirm that At4g28190 encodes the *ULT1* gene.

The complete *ULT1*-coding region was determined by EST and cDNA analysis, RT-PCR and 5′RACE. This region is 714 bp in length, and consists of three exons and two introns (Fig. 2A), encoding a predicted protein of 237 amino acids with a mass of 26.7 kDa. Genomic sequence analysis indicated the presence of a TATA box, a CCAAT box and a GC box, as well

as an in frame stop codon upstream of the transcription start site. Ceres cDNA 96705 (www.arabidopsis.org) and the sequencing of RT-PCR products support the annotation of this gene. We have identified a missense mutation in the second exon of this gene in the *ult1-1* and the *ult1-2* alleles (Fig. 2A). The *ult1-1* mutation is caused by a G to A transition that changes a cysteine residue to a threonine residue at position 173 relative to the translational initiation site (Fig. 2B). The *ult1-2* mutation is due to a C to T transition that replaces a serine residue with a phenylalanine residue at position 83.

Database searches revealed the presence of a sequence on *Arabidopsis* chromosome 2 that is highly similar to *ULT1* at the nucleotide level. This paralogous gene, At2g20825, consists of two exons and a single intron. Because overexpression of this gene can rescue the *ult1-1* mutant phenotype (see below), we refer to this locus as *ULT2*. Conceptual translation of *ULT2* gives a putative protein of 226 amino acids (26.1 kDa) with 81% identity and 86% similarity to ULT1 over the full-length of the proteins (Fig. 2B). Twenty-one of the 23 cysteine residues present in ULT1, including C173 which is mutated in the *ult1-1* allele, are conserved in the ULT2 protein. The serine residue (S83) that is mutated in the *ult1-2* allele is also conserved in ULT2. Notably, ULT1 contains five amino acids at the N terminus (residues 2-5) and six amino acids in the middle of the protein (residues 121-126) that are not present in the putative ULT2 protein.

We have identified sequences corresponding to *ULT1*- and *ULT2*-like genes in a number of other plant species, including tomato, maize, cotton, rice, soybean and wheat. So far, only a single ULT-like gene has been identified in these species, compared with two in *Arabidopsis*. An amino acid alignment of the putative ULT-like proteins for which full-length or nearly full-length genomic and/or EST sequences are available, is shown in Fig. 2B. The overall identity between the proteins ranges from 59% to 72% across the length of the protein. No functions have yet been assigned to any of these ULT-like proteins. The *ult1-1* and *ult1-2* mutations both occur in amino acids that are invariant among all nine of the plant species examined, suggesting that these residues are crucial for protein function.

Sequence analysis of the ULT1 and ULT2 proteins

Two domains can be recognized in the ULT1 and ULT2 protein sequences that have been found in transcription factors. The Prosite program (pit.georgetown.edu) revealed a significant structural homology between the N-terminal region of the ULT proteins (Fig. 2B) and a conserved SAND domain found in animal proteins. The SAND domain is an evolutionarily conserved ~80-100 amino acid DNA-binding motif that takes its name from the Sp100, AIRE-1, NucP41/75 and DEAF-1/suppressin proteins found in humans and *Drosophila melanogaster* (Gibson et al., 1998). The ULT1 and ULT2 proteins, as well as the other ULT-like plant sequences, share ~75% identity within the SAND domain (Fig. 2C).

The three-dimensional structures of several SAND domains have been determined by NMR and x-ray crystallography (Bottomley et al., 2001; Surdo et al., 2003). The SAND domain is a compact, strongly twisted α/β fold consisting of five antiparallel β-sheets alternating with four α-helices (Fig. 2C). However, the primary sequence of the SAND domain is poorly conserved between family members. The highest degree of amino acid conservation is found between two otherwise unrelated proteins from *C. elegans*, CeC25G4.4 and CeC44F1.2, which share 57% identity within the SAND domain. Most of the animal proteins share less than 30% identity within the SAND domain, and the pair-wise comparison score can be as low as 7% identity, as shown for the human AIRE-1 and GMEB1/2 proteins. Thus, the similarity between animal SAND domains instead resides at the secondary and consequent tertiary structure level. Similarly, the major conservation of the ULT SAND domains is at the level of the secondary structure: The PsiPred program (McGuffin et al., 2000) predicts the β1, β2, β3 and β5 strands, as well as the α2 and α4 helices in the ULT proteins (Fig. 2C). The program did not detect the α1 and α3 helices or the β4 sheet, probably because of their extremely small size. Only two conserved cores are highlighted by multiple alignment of the SAND domains, the TPxxFE and the KDWK motifs (Fig. 2C). The TPxxFE motif is perfectly conserved among all the putative ULT-like proteins in plants (Fig. 2B,C). The KDWK core is not conserved in ULT1 and ULT2 nor in the mouse and human AIRE-1 proteins at the primary sequence level, but the secondary structure is conserved. The *ult1-2* mutation, which causes a null mutant phenotype (see below), lies within the α2 helix of the SAND domain (Fig. 2B,C).

The ULT1 and ULT2 proteins are highly cysteine rich, with cysteine residues accounting for 9.7% of the total amino acid content of each protein (Fig. 2B). One particular arrangement of cysteine residues near the C terminus of the ULT1 and ULT2 proteins is highly similar to that of a B-box motif found in many eukaryotes (Fig. 2D). In these organisms, the B-box domain has been proposed to function in protein-protein and in protein-RNA interactions (Borden, 1998; Torok and Etkin, 2000). B-box domains are associated with cysteine-rich zinc-binding motifs in otherwise unrelated proteins, many of them transcription factors, that participate in a wide range of cellular processes (Borden, 1998; Torok and Etkin, 2000). The putative B-box region is more highly conserved between ULT1 and the homologous sequences than the rest of the protein (Fig. 2B).

Subcellular localization of the ULT proteins

In animals, SAND domain-containing proteins are found in the nucleus, in the cytoplasm, or in both compartments (Gross and McGinnis, 1996; Jimenez-Lara et al., 2000; Peterson et al., 2004). Similarly, eukaryotic proteins containing B-box domains have been localized to either the nucleus or the cytosol (Borden, 1998; Torok and Etkin, 2000). The computer programs Prosite (Hulo et al., 2004; Sigrist et al., 2002), PSORT (Nakai and Kanehisa, 1992), SignalP (Nielsen et al., 1997), and NLSdb (Nair et al., 2003) each predict the ULT1 and ULT2 proteins to be localized to the cytosol, based on the absence of any sorting or signal peptide. However, both ULT proteins are small enough to diffuse passively into the nucleus through the nuclear pores (Raikhel, 1992). Subcellular localization experiments using enhanced green fluorescent protein (EGFP) as a marker showed that ULT1-EGFP and ULT2-EGFP fusion constructs transiently transformed into onion epidermal cells are localized in both the nucleus and the cytosolic compartments (Fig. 3A).

To determine the relevance of this localization pattern in vivo, we generated transgenic *ult1-1* plants stably expressing either the ULT1-EGFP or ULT2-EGFP fusion protein under the

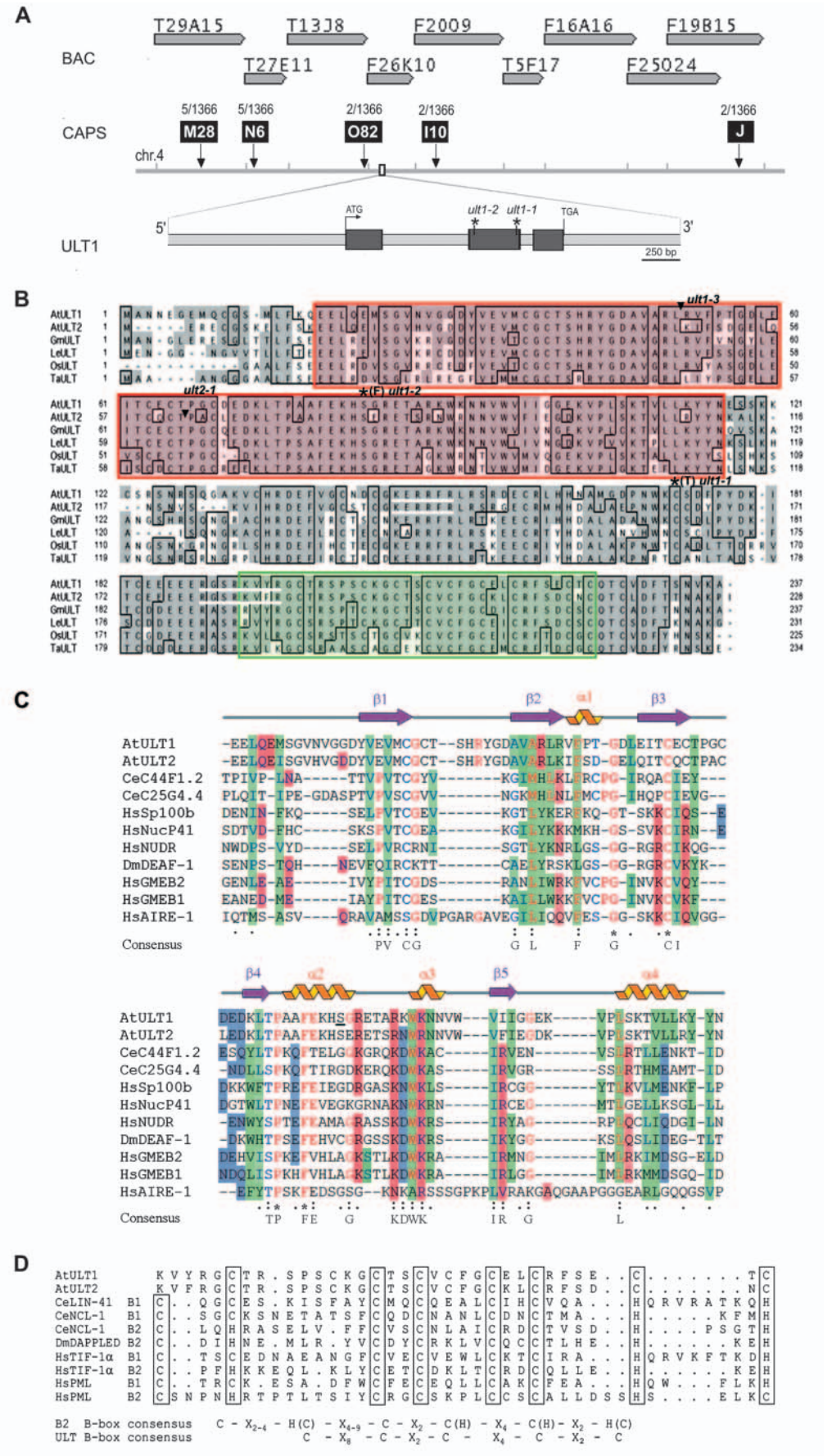
A
BAC
T29A15
T13J8
F2009
F16A16
F19B15
T27E11
F26K10
T5F17
F25O24
CAPS
5/1366
5/1366
2/1366
2/1366
2/1366
M28
N6
O82
I10
J
chr.4
ULT1
5'
3'
ATG
ult1-2
ult1-1
TGA
250 bp
B
ult1-3
ult2-1
*(E) ult1-2
*(T) ult1-1
AtULT1
AtULT2
GmULT
LeULT
OsULT
TaULT
C
β1
β2
α1
β3
β4
α2
α3
β5
α4
AtULT1
AtULT2
CeC44F1.2
CeC25G4.4
HsSp100b
HsNucP41
HsNUDR
DmDEAF-1
HsGMEB2
HsGMEB1
HsAIRE-1
Consensus
D
AtULT1
AtULT2
CeLIN-41 B1
CeNCL-1 B1
CeNCL-1 B2
DmDAPPLED B2
HsTIF-1α B1
HsTIF-1α B2
HsPML B1
HsPML B2
B2 B-box consensus C - X2-4 - H(C) - X4-9 - C - X2 - C(H) - X4 - C(H) - X2 - H(C)
ULT B-box consensus C - X8 - C - X2 - C - X4 - C - X2 - C

Fig. 2. *ULTRAPETALA1* cloning and sequence analysis. (A) Schematic of the positional cloning of the *ULT1* locus and the structure of the *ULT1* gene. The region of chromosome 4 containing BACs T29A15 to F19B15 is represented. The CAPS markers designed for mapping *ult1-2* are shown in black boxes and the frequency of recombinant chromosomes is indicated for each marker. The exon/intron structure of the *ULT1* gene is shown along with the positions of the *ult1-1* and *ult1-2* mutations. (B) Alignment of the conceptual translation products of the Arabidopsis *ULT1* and *ULT2* genomic sequences with conceptually translated consensus EST sequences from four other plant species. The sequences compared are from *Arabidopsis thaliana* ULT1 (AtULT1, At4g28190), *Arabidopsis thaliana* ULT2 (AtULT2, At2g20825), *Glycine max* (GmULT, BM524875.1), *Lycopersicon esculentum* (LeULT, EST357945), *Oryza sativa* (OsULT, CA763280.1) and *Triticum aestivum* (TaULT, BG604592). Identical amino acids are boxed and blocks of similar amino acid residues are shaded. The positions of the mutations in ULT1 and ULT2 are shown above the sequences, the SAND domain is boxed in red and the B box-like motif is boxed in green. Stars indicate the amino acid substitution in the *ult1-1* (C173T) and *ult1-2* (S83F) alleles. Arrowheads denote the position of the T-DNA insertion in the *ult1-3* and the *ult2-1* allele. Arginine/lysine rich nuclear localization signal (NLS) candidate polypeptides are underlined in white. (C) Multiple sequence alignment of AtULT1, AtULT2 and animal SAND domains from CeC44F1.2 (*Caenorhabditis elegans*, Z49067), CeC25G4.4 (*Caenorhabditis elegans*, Z70680), HsSp100b (*Homo sapiens*, U36501), HsNucP41 (*Homo sapiens*, Q14976), HsNUDR (*Homo sapiens*, AF049459), DmDEAF-1 (*Drosophila melanogaster*, AAC47040), HsGMEB2 (*Homo sapiens*, NM031803), HsGMEB1 (*Homo sapiens*, NM006582), AIRE-1 (*Homo sapiens*, AB006682). The alignment was obtained with the ClustalW 1.82 program and manually refined using the calculated two-dimensional structure. Secondary structure elements are shown above the multiple alignment. Period, semicolon and asterisk mark partial to full residue conservation. Color-coding reflects the conservation of amino acid types. Background colors reveal their physiochemical properties (green: hydrophobic; red: positively charged residues; blue: negatively charged residues), while foreground colors mark identical (red) and similar (blue) amino acids. The amino acid corresponding to the position of *ult1-2* mutation is underlined. (D) Alignment of the AtULT1 and AtULT2 B box-like domains with B-box proteins from animals: CeLIN-41 (*Caenorhabditis elegans*, NP492488), CeNCL-1 (*Caenorhabditis elegans*, P34611), DmDAPPLED (*Drosophila melanogaster*, Q9V4M2), HsTIF-1 α (*Homo sapiens*, NP003843), HsPML (*Homo sapiens,* P29590). The conserved cysteine/histidine residues are boxed. Below the sequence alignment, the conserved spacing of the B2 B-box consensus (Torok and Etkin, 2000) and the ULT B-box consensus are compared.

control of the 35S promoter. Transgenic plants that expressed the ULT1 or ULT2 protein with the EGFP moiety attached to either the N terminus or the C terminus had a wild-type appearance, indicating that the fusion proteins are functional in either orientation and can rescue the *ult1-1* mutant phenotypes. Visualizing the ULT1-EGFP or ULT2-EGFP fusion proteins in the roots or petals of the transgenic plants, we observed signal in both the nucleus and the cytosol (Fig. 3B-D). Immunoblotting of extracts from the transgenic plant using an anti-GFP antibody showed that the observed localization pattern is not an artifact due to the cleavage of the fusion protein (Fig. 3E). The same ULT-EGFP fusion proteins in combination with a nuclear localization signal (NLS) or a nuclear export signal (NES) also complement the mutant phenotype when expressed in an *ult1-1* background (data not shown).

However, as the ULT-EGFP fusion proteins are still smaller than the nuclear pore exclusion size they may enter or exit the nucleus passively, especially when expressed at high levels under the 35S promoter. To prevent passive entry into or exit from the nucleus, we fused each ULT protein to a combined GUS (β-glucuronidase)-EGFP protein (Grebenok et al., 1997). When bombarded into onion epidermal cells, the constructs gave a GFP and a GUS signal primarily in the cytosol for some cells and equivalently in the cytosol and the nucleus for others (Fig. 3F,G). Thus, the ULT1 and ULT2 proteins have a dual localization in the nucleus and in the cytosol, and may function in both compartments.

ULT1 and *ULT2* expression analysis

We used RT-PCR to determine the distribution of *ULT1* and *ULT2* mRNA transcripts in wild-type tissues. As shown in Fig. 4, *ULT1* transcripts could be amplified from all tissues tested: roots, 8-day-old seedlings, mature leaves, stems, inflorescences, pollen and siliques. *ULT2* expression was specific to the reproductive developmental stage, being detected only in inflorescences, pollen and siliques. For both genes, the highest level of expression was observed in inflorescence tissues.

We then performed in situ hybridization experiments to localize the *ULT1* and *ULT2* mRNAs more precisely in the tissues where they could be detected by RT-PCR. *ULT1* and *ULT2* transcripts can be detected throughout the inflorescence meristem, and a weak signal can also be detected in the inflorescence vascular tissues (Fig. 5A,B). Neither *ULT1* nor *ULT2* transcripts are detectable in stage 1 flower meristems budding from the flanks of the inflorescence meristem, but they reappear much stronger in late stage 2 primordia. As soon as the sepal primordia initiate (stage 3), *ULT1* and *ULT2* expression is excluded from these organ primordia and becomes restricted to the floral meristem (Fig. 5B). As flower development continues, *ULT1* and *ULT2* transcripts become further restricted to stamen and carpel primordia (Fig. 5D-G). Expression in carpels was detected only in the adaxial domain, corresponding to the region of ovule formation. Hybridization to cross-sections of mature flowers reveals specific signal throughout the ovules and in the tapetum tissue of the anthers (Fig. 5H-I). Thus, the *ULT1* and *ULT2* mRNA expression patterns are coincident in inflorescence meristems, floral meristems and developing flowers.

Next, we determined the expression patterns of both genes in seedlings and embryos. *ULT1* is expressed throughout the vegetative SAM and in young leaf primordia (Fig. 6A). A stronger *ULT1* signal is detected on the adaxial side of the leaf primordia, as observed for the carpel primordia. The antisense *ULT2* mRNA probe did not hybridize to seedling tissues (Fig. 6B), confirming that *ULT1* but not *ULT2* is expressed during the vegetative stage. In mature embryos, both *ULT1* and *ULT2* transcripts are detected in the SAM, and *ULT2* expression is also observed in the RAM (Fig. 6D-G). The expression is detected in very restricted domains corresponding to meristematic cells localized at the apices. Interestingly, in all

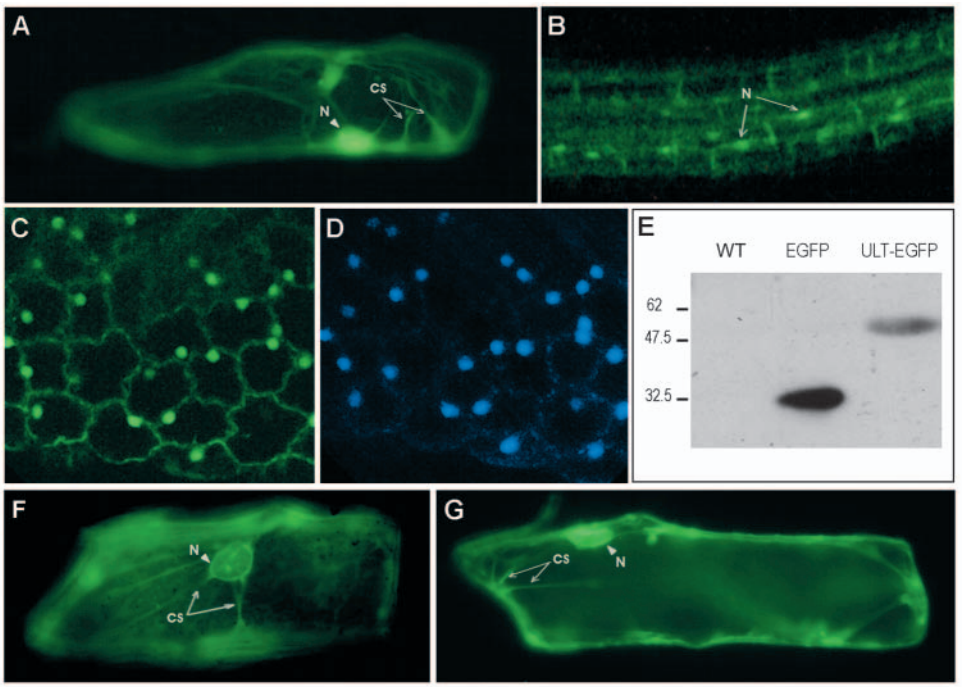

Fig. 3. Subcellular localization of the ULT proteins. (A) Dark-field exposure of an onion epidermal cell transiently expressing an ULT1-EGFP fusion protein. The GFP signal is detected in both the nucleus (arrowhead) and the cytosol. In the cytosol, the fusion protein appears to be distributed in cytoplasmic streams (arrows). (B) Confocal image of a root from a 35S::ULT1-EGFP T2 transgenic plant. (C,D) Confocal image of a petal from a 35S::ULT1-EGFP T2 transgenic plant. (D) DAPI staining of the nuclei and cell walls in the petal shown in C. (E) An immunoblot of protein extracts from inflorescence meristem tissue, using anti-GFP serum. WT, extract from a wild type L*er* plant; EGFP, extract from a 35S:EGFP transgenic plant; ULT-EGFP, extract from a 35S::ULT1-EGFP T2 transgenic plant. (F,G) Dark-field exposures of onion epidermal cells transiently expressing the ULT1-GUS-EGFP fusion protein. The GFP signal is detected in the cytosol and the perinuclear region (F) or both in the cytosol and throughout the nucleus (G). N, nucleus; CS, cytoplasmic streams.

earlier analyzed stages – from the eight-cell stage to the bending cotyledon stage – *ULT1* and *ULT2* transcripts are localized throughout the embryo, occasionally displaying a stronger signal between the developing cotyledons and in the vasculature (Fig. 6J-P). This suggests that ULT expression becomes tissue-restricted only at the time when the embryo enters the maturation phase of development. No signal was detected in the suspensor or in the endosperm at any stage (Fig. 6J-P), showing that *ULT1* and *ULT2* gene expression is embryo specific.

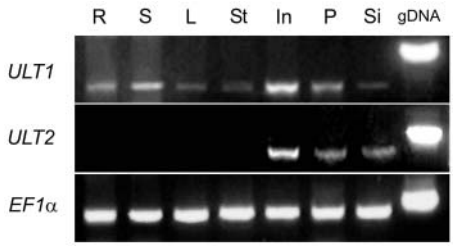

Fig. 4. Expression profiles of the *ULT1* and *ULT2* genes. RT-PCR analysis was performed on RNA extracts from various wild type L*er* tissues: roots (R), 8-day-old seedlings (S), mature rosette leaves (L), stems (St), inflorescence apices (In), pollen (P) and siliques (Si). *ULT1* transcripts were amplified from all tissues examined, whereas *ULT2* transcripts were detected only during the reproductive phase in inflorescences, pollen and siliques. *EF1α* was amplified as a control. In addition, control amplification reactions were run with each set of primers using genomic DNA (gDNA) as a template.

ULT2 overexpression can rescue the *ult1-1* mutant phenotypes

Because the *ULT1* and *ULT2* gene expression patterns overlap in inflorescence and floral meristems, we asked if ULT2 could mimic ULT1 function in these tissues. We transformed a d35S::ULT2 sense construct into *ult1-1* plants, in order to increase the level of *ULT2* expression in this mutant background. We analyzed the capacity of the d35S::ULT2 transgene to rescue the *ult1-1* phenotypes, and compared its effects with those of a d35S::ULT1 transgene, by scoring floral organ number and flowering time.

Transgenic d35S::ULT plants display a gradient of phenotypes that correlates with the level of ULT gene overexpression. Those plants expressing the highest levels of *ULT1* or *ULT2* show dramatic vegetative phenotypes as soon as a few days after germination (C.C.C. and J.C.F., unpublished). Consequently, we performed the complementation analysis on d35S::ULT2 *ult1-1* lines that had a wild-type appearance at the vegetative stage. As expected, RT-PCR experiments showed that these lines display a more moderate increase in *ULT2* gene expression than the dramatically affected overexpression lines (data not shown). By analyzing these moderate overexpression lines, we found that the d35S::ULT2 transgene complements the *ult1-1* mutant phenotypes to the same extent as the d35S::ULT1 transgene (Fig. 7). Indeed, *ult1-1* plants containing either of these constructs display floral organ number and bolting time phenotypes close to those of the wild type. Thus, although the

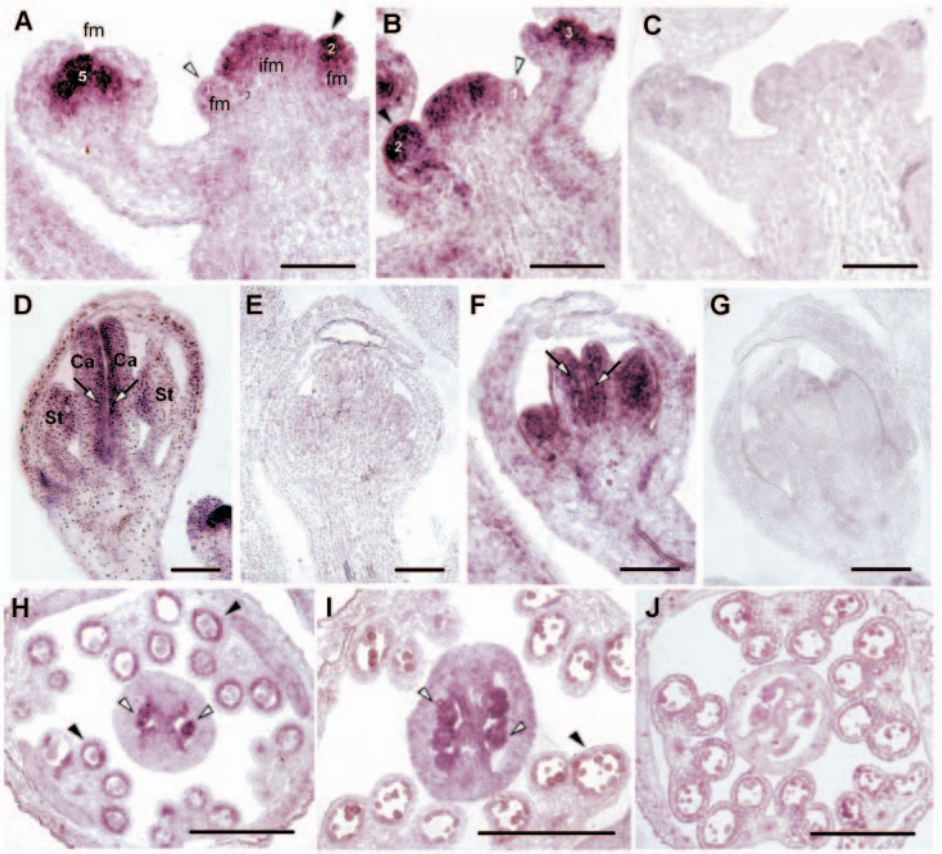

Fig. 5. *ULT1* and *ULT2* mRNA expression patterns in inflorescence and flower tissues. RNA localization by in situ hybridization with *ULT1* (A,D,H) and *ULT2* (B,F,I) antisense probes hybridized to wild-type L*er* tissues. (A-C) Longitudinal sections through the inflorescence meristem (ifm) and adjacent floral meristems (fm). *ULT1* mRNA is localized throughout the inflorescence meristem. No signal was detected in stage 1 floral meristems (white arrowheads). *ULT1* transcripts reappeared in late stage 2 floral primordia (black arrowheads). As soon as the sepals initiate (stage 3 flower), *ULT1* expression becomes restricted to the center of the floral meristem. (C) Control hybridization with an *ULT2* sense probe. (D-G) Longitudinal sections through stage 7-8 flowers. *ULT1* (D) and *ULT2* (F) mRNA was detected in stamen (St) and carpel (Ca) primordia. In both cases the signal appears stronger on the adaxial side of the carpels (arrows). (E,G) Control hybridizations with *ULT1* and *ULT2* sense probes. (H-J) Transverse sections through mature flowers. *ULT1* (H) and *ULT2* (I) mRNA was detected in ovules (white arrowheads) and tapetum tissue in the anthers (black arrowheads). (J) Control hybridization with an *ULT1* sense probe. Scale bars: 50 μm.

endogenous level of *ULT2* is not sufficient to overcome the effect of the *ult1-1* mutation, an increase in the amount of wild-type ULT2 protein in the *ult1-1* background allows complete rescue of the *ult1-1* mutant phenotypes. These data indicate that, when expressed at higher levels, wild-type ULT2 protein can functionally compensate for mutant ULT1-1 protein.

Identification of *ult1* and *ult2* T-DNA alleles

In order to examine the full spectrum of biological functions for *ULT1* and *ULT2*, we have obtained an insertion allele of each gene. The *ult1-3* allele contains a T-DNA insertion in the first exon of *ULT1*, 155 bp after the start codon (Fig. 2B). RT-PCR experiments show that *ult1-3* plants do not accumulate *ULT1* transcripts (Fig. 8A) and place the *ult1-3* allele as a null allele. The inflorescence and flower phenotypes of plants carrying the *ult1-3* mutation are indistinguishable from those of *ult1-2* plants (Fig. 1C,D, Fig. 8B), indicating that the *ult1-2* EMS line is a phenotypic null allele probably because of the lack of functional ULT1 protein. *WUS* molecular marker analysis confirms that the *ult1-3* allele phenocopies the *ult1-2* allele (Fig. 1K,L). In *ult1-3* inflorescences, the mean organizing center size is 7.62±0.48 cells in width, 3.12±0.33 cells in height, and 18±1.22 cells in total. These values are not significantly different from *ult1-2* (Fig. 1P). Surprisingly, the *ult1-1* EMS mutation has a more severe effect on inflorescence meristem size, *WUS* domain expansion and floral organ number than either the *ult1-2* or the *ult1-3* null mutations (Fig. 1B-D,J-L,P; Fig. 8B). In addition, *ult1-2* and *ult1-3* mutant plants flower only two days later than the wild type (Fig. 8C), whereas *ult1-1* plants are more dramatically affected, flowering up to 2 weeks later than wild-type plants.

The *ult2-1* allele contains a T-DNA insertion in the intron of *ULT2*, 408 bp after the start codon. Because a weak band corresponding to correctly-spliced *ULT2* cDNA could be amplified from inflorescence tissues from some homozygous mutant individuals after 45 cycles of RT-PCR, we cannot conclude that *ult2-1* is a null allele (Fig. 8A). *ult2-1* mutant plants do not display any inflorescence or flower phenotypes, and are indistinguishable from wild-type plants (data not shown). Determining whether the presence of ULT2 protein is required for proper reproductive meristem activity will rely on the identification and analysis of a true null allele for the *ULT2* locus.

The ULT1-1 mutant protein has semi-dominant effects

Because the *ult1-1* mutant phenotype is more dramatic than that of the *ult1-3* null mutant, we analyzed the effect of the *ult1-1* mutation in the heterozygote state. *ult1-1* behaves as a slight semi-dominant allele when heterozygous: of 18 *ult1-1/+* plants scored, five had five sepals and/or petals in the first one or two flowers and one had six petals in the first flower. All *ult1-1/+* plants are wild type with respect to stamen and carpel number and floral determinacy, indicating that the *ult1-1* mutation is recessive with respect to these traits.

To test whether the semi-dominant effect of the ULT1-1 mutant protein is altered in the absence of wild-type ULT1 protein, we compared the floral organ number and flowering

time phenotypes of *ult1-1*/+ plants with those of *ult1-1/ult1-3* plants. We found that *ult1-1/ult1-3* plants are more severely affected than either *ult1-3* homozygous plants or *ult1-1*/+ heterozygous plants with respect to sepal/petal number and also flowering time (Fig. 8D,E). Thus, eliminating wild-type ULT1 protein enhances the effects of the *ult1-1* mutation on flowering time and on floral organ number in the outer two whorls.

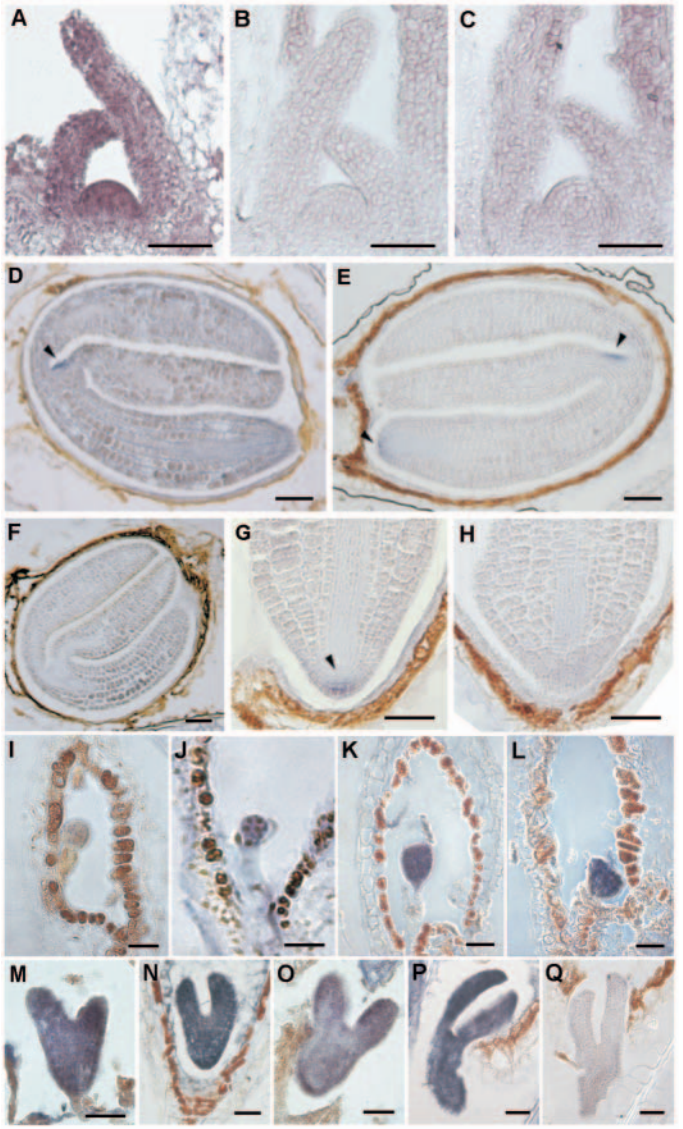

Fig. 6. *ULT1* and *ULT2* mRNA expression patterns in seedlings and embryos. RNA localization by in situ hybridization with *ULT1* (A,D,J,K,N,P) and *ULT2* (B,E,G,L,M,O) antisense probes hybridized to wild-type L*er* seedlings (A-C) and embryos (D-Q).
(A-C) Longitudinal sections through 7-day-old seedlings. (A) *ULT1* transcripts are localized throughout the vegetative SAM and in young leaf primordia. (B) *ULT2* transcripts are not detected in seedlings. (C) Control hybridization with an *ULT1* sense probe.
(D-H) Longitudinal sections through mature embryos. (D) *ULT1* expression is restricted to the embryonic SAM (arrowhead). (E) *ULT2* transcripts can be detected in the embryonic SAM and RAM (arrowheads). (G) Higher magnification of *ULT2* expression in the RAM. (F,H) Control hybridization with *ULT1* and *ULT2* sense probes, respectively. (I-Q) Longitudinal sections through embryos at different stages of embryogenesis. (I) Early globular stage. (J) Eight-cell-stage embryo. (K) Late triangle stage. (L) Early heart stage. (M) Late heart stage. (N) Early torpedo stage. (O) Torpedo stage. (P,Q) Bending cotyledon stage. (I,Q) Control hybridizations with an *ULT1* sense probe. Scale bars: 50 μm in A-F; 25 μm in G-Q.

Down-regulation of both ULT genes leads to early arrest of the vegetative SAM

Antisense plants carrying a d35S::ULT1 AS construct generated in the L*er* wild-type background show a dramatic reduction in the level of both *ULT1* and *ULT2* transcripts (Fig. 9A). Some plants from the antisense lines fail to germinate (data not shown), while the rest display a range of shoot and floral meristem defects (Fig. 9B-I).

The most strongly affected plants have severely disorganized SAMs that resemble those of *fas1* or *fas2* plants (Leyser and Furner, 1992; Kaya et al., 2001), with highly aberrant lateral organ initiation (Fig. 9B). Although L*er* wild-type seedlings develop four true leaves after 7 days of development, ULT AS seedlings have formed only two cotyledons (class 1), two barely developed filamentous leaves (class 2) or two to three stunted leaves (class 3) after 14 days of development (Fig. 9B, first row). The wild-type SAM is a dome-shaped structure that produces lateral organs in a regular phyllotaxy, but no meristematic structure can be detected between the two cotyledons of class 1 ULT AS plants (arrowhead). Class 2 plants initiate leaf primordia at a greatly reduced rate and their SAMs are very small and flat (asterisk), while class 3 plants produce small leaf primordia (arrowheads) around a reduced SAM composed of few enlarged cells (Fig. 9B, second row). Comparison of sections through 7-day-old L*er* and 14-day-old ULT AS seedlings (Fig. 9B, third row) shows that class 1 and class 2 AS seedlings lack more than a few meristematic cells (arrowheads). Sections through class 3 ULT AS shoot apices reveal a small group of enlarged cells that are not organized into layers as in the wild type. After the termination of the primary SAM some ULT AS plants initiate axillary meristems, which generate one or more inflorescences (Fig. 9D) much later than wild-type plants (Fig. 9C). These axillary inflorescence meristems can also arrest precociously, after the production of a couple of flowers (Fig. 9E).

The least severely affected ULT AS plants produce flowers that resemble those of *ult1-2* mutants (Fig. 9F-I). These plants form flowers with supernumerous floral organs (Fig. 9G) when compared with wild-type plants (Fig. 9F). Five sepals and five petals are observed in some flowers (Fig. 9G), and others form up to four carpels (Fig. 9H). Flowers from the ULT AS lines also display a partial loss of determinacy, in that supernumerous carpels can develop as fifth whorl structures within the fourth whorl gynoecium (Fig. 9I, arrow).

Discussion

ULT1 regulates the size of the inflorescence meristem organizing center

It has been well established that the self-perpetuation of shoot and floral meristems requires interactions between the *CLV* and *WUS* factors, which set up a feedback loop between the stem cells and the underlying organizing center (Brand et al., 2000; Schoof et al., 2000). When the negative regulation of meristem cell accumulation is disrupted in *clv* mutants the *WUS*

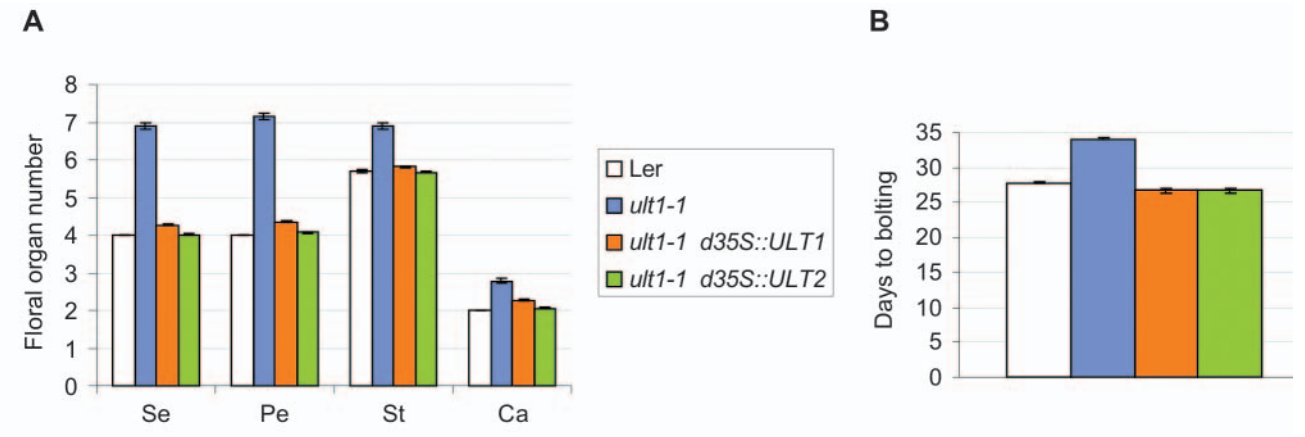

Fig. 7. Rescue of the *ult1-1* mutant phenotype by an *ULT2* transgene. (A) Floral organ number in wild-type L*er* plants, *ult1-1* plants and *ult1-1* plants containing the d35S::ULT1 or d35S::ULT2 construct. Graph shows the mean number of organs in the first ten flowers of 10 plants (n=100 flowers), and the standard error is indicated. For the transgenic lines in the *ult1-1* mutant background, the mean organ number was calculated from the first ten bolting T1 plants that did not show an overexpression phenotype. (B) Days to bolting after germination for L*er* plants, *ult1-1* plants and *ult1-1* plants containing the d35S::ULT1 or d35S::ULT2 construct. The mean number of days to bolting was calculated from the same populations of plants that were used for the floral organ counts in (A) (n=10 plants), and the standard error is indicated.

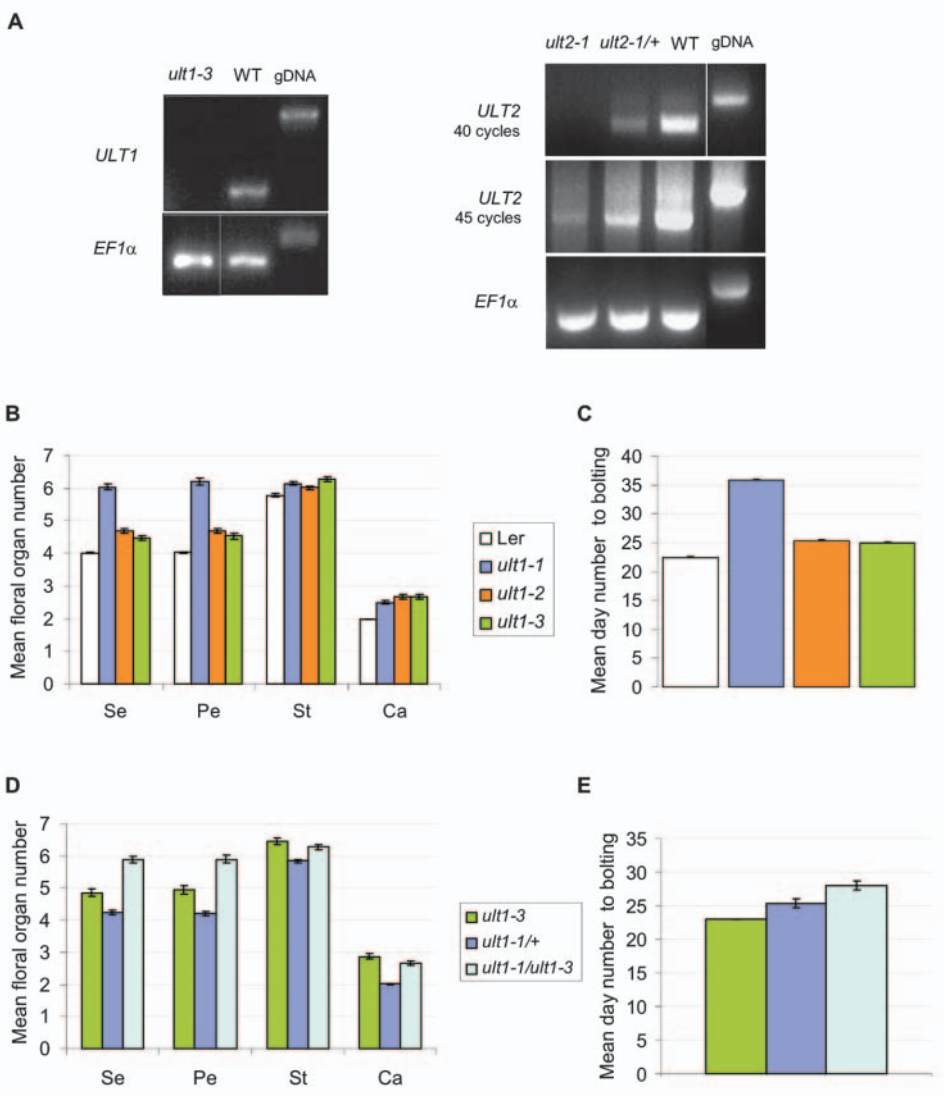

Fig. 8. *ULT1* and *ULT2* T-DNA insertion alleles. (A) RT-PCR on wild type L*er*, *ult1-3* and *ult2-1* T-DNA insertion mutant inflorescences. *ULT1* transcripts could be amplified from L*er* (wild-type) plants but not from *ult1-3* plants, while *ULT2* transcripts were detected in wild-type Col-0 and *ult2-1*/+ heterozygous plants but not in *ult2-1* homozygous plants after 40 cycles of PCR. However, after 45 cycles a faint signal corresponding to correctly spliced *ULT2* transcript was detected in the *ult2-1* homozygous lane. *EF1*α was amplified as a control. Additional control amplification reactions were run with each set of primers using genomic DNA (gDNA) as a template. (B) Floral organ number in L*er*, *ult1-1*, *ult1-2* and *ult1-3* mutant plants. Graph shows the mean number of organs in the first ten flowers of 10 plants (n=100 flowers), and the standard error is indicated. (C) Mean days to bolting after germination for L*er*, *ult1-1*, *ult1-2* and *ult1-3* plants (n=10 plants). The standard error is indicated. (D) Floral organ number in *ult1-3* homozygous plants, *ult1-1*/+ heterozygous plants and *ult1-1*/*ult1-3* plants. Graph shows the mean number of organs in the first ten flowers of four or six plants (n=40 flowers for *ult1-3* and n=60 flowers for the other genotypes), and the standard error is indicated. (E) Mean days to bolting after germination for *ult1-3* homozygous plants, *ult1-1*/+ heterozygous plants and *ult1-1*/*ult1-3* plants (n=4 plants for *ult1-3* and n=6 flowers for the other genotypes). The standard error is indicated.

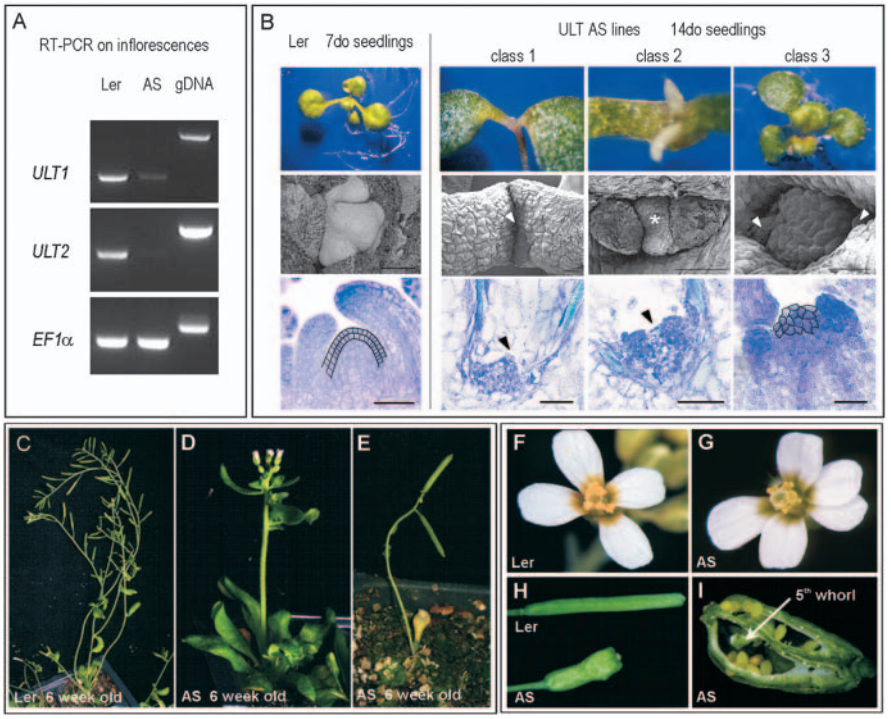

Fig. 9. Phenotypes of ULT antisense (AS) lines. (A) RT-PCR on inflorescences of the least affected ULT AS plants (those showing the flower phenotypes illustrated in G-I). The expression of both *ULT1* and *ULT2* is downregulated. *EF1α* was amplified as a control. (B) Vegetative phenotypes of the most severely affected ULT AS lines. The plants were grouped into three classes based on their SAM termination phenotypes (class 1 plants terminate the earliest). Shoot apex bright-field images (first row), SEM images (second row), and longitudinal sections (third row) are shown for 7-day-old wild-type L*er* seedlings and 14-day-old ULT AS seedlings. (C-E) Reproductive phenotypes of the ULT AS lines. (C) Six-week-old L*er* plants. (D,E) Six-week-old ULT AS plants showing reduced flower number and premature arrest of the axillary inflorescence meristems. (F-I) Flower phenotypes of the least affected ULT AS lines. (F) L*er* flower. (G) ULT AS flower with extra sepals and petals. (H) Siliques from a L*er* flower and from an ULT AS flower with extra carpels. (I) Silique from an ULT AS flower dissected open to reveal the presence of a fifth whorl carpeloid structure developing inside the fourth whorl (arrow). Scale bars: 20 μm.

expression domain expands laterally and upwards, correlating with an increase in stem cell accumulation and meristem fasciation (Brand et al., 2000). Our analysis in *ult1* mutant plants of molecular markers for different meristem regions indicates that like the CLV proteins, ULT1 also plays a role in preventing the lateral enlargement of the *WUS*-expressing cell population in reproductive meristems. In the absence of ULT1 function, the increased number of cells in the central region of the meristem may enable the production of extra floral primordia from the inflorescence meristem and extra organ primordia from the floral meristem.

Several observations suggest that ULT1 and the CLV loci regulate the size of the *WUS*-expressing cell population via separate pathways. First, the meristems of *clv* mutant plants, but not of *ult1* mutant plants, are measurably taller than those of wild-type plants (Clark et al., 1993; Clark et al., 1995; Fletcher, 2001). Second, in *clv* but not in *ult1* inflorescence meristems the *WUS* expression domain extends one cell layer up compared with wild type. Third, *ult1* and *clv* alleles show synergistic effects on inflorescence and floral meristem size, suggesting that they use separate pathways to regulate a common process (Fletcher, 2001). Finally, although *wus* mutations have been shown to be epistatic to *clv* mutations in both shoot and floral meristems, *ult1 wus* double mutants have additive phenotypes, except in the center of the flower (Carles et al., 2004). Thus, ULT1 has both *WUS*-dependent and *WUS*-independent functions in maintaining meristem activity, and converges with the CLV pathway primarily at the point of limiting the lateral expansion of the *WUS*-expressing cell population.

ULT1 and ULT2 proteins resemble transcriptional regulators

ULT1 and ULT2 define a small family of closely related plant proteins that contain conserved SAND and B box-like domains. A high degree of sequence conservation between the *Arabidopsis* ULT1 and ULT2 proteins and predicted proteins in eight other monocot and dicot species was observed across the length of the proteins (Fig. 2B). In addition, the ULT-like ESTs from tomato, soybean and alfalfa were identified from shoot and/or floral meristem tissues – tissues in which *Arabidopsis* ULT1 is known to act (Carles et al., 2004; Fletcher, 2001). This observation suggests that the roles ULT1 plays in meristem maintenance and floral determinacy may be widely conserved among angiosperms.

Until now, reports of proteins containing a SAND domain have been restricted to the animal phyla (Bottomley et al., 2001; Gibson et al., 1998; Surdo et al., 2003). Overall, their primary sequences are quite divergent except for two core elements, but the secondary structure of the SAND domain is highly conserved. The same holds true for the SAND domains present in ULT1 and ULT2. The *ult1-2* missense mutation, which lies in the α2 helix of the ULT1 SAND domain, changes a serine residue to a phenylalanine. In other SAND domain proteins glycine, alanine or cysteine residues are encountered at the same position. These amino acids, like serine, have small side chains. Thus, the introduction of a highly hydrophobic aromatic phenylalanine residue is likely to disrupt the structure of the SAND domain in the mutant ULT1-2 protein, perturbing potential DNA-binding and/or protein-protein interactions. Moreover, the fact that such a missense mutation behaves as a knockout mutation illustrates the importance of the SAND domain in ULT1 protein function.

Many SAND domain-containing proteins, such as DmDEAF-1, HsNUDR and HsGMEB1/2, have been shown to bind specifically to DNA (Bottomley et al., 2001; Burnett et al., 2001; Gross and McGinnis, 1996; Surdo et al., 2003). The SAND domain itself has been proven to mediate this interaction via the KDWK motif-containing region (Bottomley et al., 2001; Jimenez-Lara et al., 2000; Surdo et al., 2003). Moreover, the SAND domain has been shown to be necessary

for the transactivation and homo-multimerization activities of AIRE (Halonen et al., 2004), as well as for its nuclear localization (Ramsey et al., 2002). Altogether, phenotypic and biochemical studies, along with three-dimensional structure modeling, suggest that the SAND domain defines a novel DNA-binding module involved in the regulation of gene transcription. The cloning of the *ULT1* gene has led us to the identification of a novel group of plant SAND domain proteins with a conserved secondary structure. By analogy with animal SAND domain factors, we propose that ULT1 and ULT2 may function as transcription regulators, possibly binding directly to target DNA. Alternatively, association of the ULT proteins with DNA might require the presence of a liaison factor between the SAND domain and the target DNA sequence, as observed for the AIRE protein (Pitkänen et al., 2001).

Our subcellular localization studies show that the ULT1 and ULT2 proteins accumulate in, and may be functional in, both the nucleus and the cytosol. One possibility for this dual localization pattern is that the small ULT proteins diffuse freely between the nucleus and the cytoplasm. However, when we generated ULT-GUS-EGFP fusion proteins that were too large to passively enter the nucleus, we still detected signal in the nuclear compartment. This implies that the ULT proteins either contain a functional NLS for nuclear import, or that they enter the nucleus by forming complexes with protein partners that possess an NLS core (Boulikas, 1994). A canonical NLS is not detected in the ULT proteins, but both the ULT1 and ULT2 sequences contain a hexapeptide and an octapeptide that each has four arginine or lysine residues. These sequences may correspond to nuclear targeting signals or be part of a bipartite NLS core (Hicks and Raikhel, 1995), as reported for the AIRE protein (Pitkänen et al., 2001). The dual nuclear and cytoplasmic localization of ULT1 and ULT2 proteins is not unprecedented among the SAND domain-containing proteins (Halonen et al., 2004; Ramsey et al., 2002). One possibility is that the dual localization in the nucleus and the cytosol may serve as a modulation mechanism for transcriptional regulation, as shown for some families of transcription factors in plants and animals (Fabbro and Henderson, 2003; Merkle, 2001; Ziegelbauer et al., 2001).

ult1-1 is a dominant negative allele

Side-by-side comparison of *ult1-2* and *ult1-3* homozygous plants showed that their phenotypes are indistinguishable from one another, revealing that *ult1-2* is a phenotypic null allele for the *ULT1* locus. However, the *ult1-1* EMS allele confers a more severe phenotype than the other two alleles with respect to sepal/petal number and flowering time. Analysis of heterozygous *ult1-1*/+ plants shows that the *ult1-1* mutation is semi-dominant with respect to these traits. When we scored for *ult1-1* semi-dominancy in an *ult1-1*/*ult1-3* hemizygous background, we found that the effect of the ULT1-1 mutant protein was more dramatic when wild-type ULT1 protein was absent. In fact, *ult1-1*/*ult1-3* plants closely resembled *ult1-1*/*ult1-1* plants. These results suggest that in *ult1-1*/+ heterozygous plants, wild-type ULT1 protein can compete with the mutant ULT1-1 protein and maintain some normal function, whereas in *ult1-1*/*ult1-3* plants no wild-type ULT1 protein is present to compete with the dysfunctional ULT1-1 mutant protein.

It is possible that the *ult1-1* missense mutation abolishes protein function but does not prevent binding to other factors. In such a scenario, ULT1-1 mutant protein would compete with wild-type ULT1 protein, sequestering one or more physical interaction partners and preventing or altering their activity. As the *ULT1* and *ULT2* expression patterns fully overlap in the inflorescence, it is possible that the two proteins themselves physically interact. The example of the SAND domain proteins GMEB-1 and GMEB-2, which share a high amino acid similarity and interact with one another in vitro (Jimenez-Lara et al., 2000), is consistent with this idea. In the *ult1-1* allele, ULT1-1 mutant protein could sequester wild type ULT2 protein, preventing ULT2 from functioning in shoot and flower tissues. However, because *ULT1* and *ULT2* expression patterns do not fully overlap throughout development, it seems likely that the ULT proteins also interact with additional factors.

Roles of the *ULT1* and *ULT2* genes in development

The phenotypes displayed by *ult1* null mutant plants reveal that *ULT1* plays an important role in negatively regulating inflorescence and floral meristem size, and in maintaining floral meristem determinacy (Carles et al., 2004; Fletcher, 2001). Correspondingly, we find that the *ULT1* gene is expressed in inflorescence meristems, floral meristems and developing carpels. Yet despite its role in negatively regulating the size of the *WUS*-expressing organizing center in a central and interior domain, *ULT1* is expressed throughout the shoot and floral meristems, similar to *STM*, rather than in a region-specific fashion like *CLV3, CLV1* and *WUS*. These data suggest that ULT1 may interact with other, as yet unidentified region-specific factors in the meristem to restrict the accumulation of the *WUS*-expressing cell population. Moreover, the fact that *ULT1* is expressed in other domains, such as cotyledon and leaf primordia, shows that ULT activity is not restricted to the meristems. The expression of *ULT1* in the developing tapetum and ovules, in particular, implies a specific function(s) in reproduction. However, the absence of detectable phenotypes outside the shoot and floral meristems in *ult1* mutant plants again suggests redundancy with other factors, such as *ULT2*.

The pattern of *ULT2* expression in inflorescence meristems, floral meristems and developing flowers appears to coincide perfectly with that of *ULT1*, yet *ult2-1* T-DNA mutant plants do not display any shoot or floral phenotypes. Currently, we cannot exclude the possibility that the presence of very low levels of ULT2 protein translated from rare correctly spliced transcripts is sufficient for proper reproductive meristem activity in the *ult2-1* mutant. Nonetheless, the presence of wild-type levels of ULT2 cannot compensate for the loss of ULT1 activity in reproductive meristems, whereas increasing *ULT2* expression under the control of a dual 35S promoter can complement the *ult1-1* mutation. This observation positions ULT2 as a functional duplicate of ULT1, and suggests that shoot and floral meristem activity may be sensitive to the dose of the ULT proteins. The necessity to fine tune the regulation of genes involved in meristem maintenance could explain the retention of both ULT factors in *Arabidopsis*. This implies that ULT1 and ULT2 are likely to have multiple common targets, the regulation of which is dependent on ULT dose. That the two genes have other independent targets, as well, is clear from the specific expression of *ULT1* in leaf primordia and *ULT2* in the embryonic root apical meristem.

ULT1 and *ULT2* transcripts are detected throughout the

embryo as early as the octant stage, and continue to accumulate in all cells of the embryo proper until maturity, when *ULT1* transcripts become restricted to the SAM and *ULT2* transcripts to the SAM and RAM. To our knowledge, *ULT1* and *ULT2* encode the only mRNAs characterized thus far that become restricted to the meristems at such a late stage of embryo maturation. The high level of *ULT1* and *ULT2* expression throughout the developing embryo might be a sign that these genes have important functions early in development that are not revealed in the single mutants. Our previous results have shown that *ult1* mutations restore SAM activity to *stm* and *wus* null mutant seedlings (Carles et al., 2004), indicating that *ULT1* functions to restrict SAM cell accumulation prior to the appearance of a visible phenotype in *ult1* mutant plants. Our analysis of *ULT1/ULT2* antisense lines provides additional evidence for an early and important function for the ULT genes, as downregulation of both *ULT1* and *ULT2* can result in aberrant lateral organ production and SAM arrest very early during seedling development.

We thank Chris Day for providing the pCD214 and pCD223 plasmids, David Ehrhardt for the pEZS vectors, and Anita Fernandez and Kathy Barton for the pSTM::GUS line. We also thank Harley Smith and George Chuck for advice concerning the in situ procedure, Doris Kim and Kristen Kwan for assistance with the subcellular localization experiments, Steve Ruzin and Denise Schichnes for help with the confocal microscopy, Guillaume Blanc for thoughtful discussions, and Sheila McCormick, Karen Osmont and Leor Williams for helpful comments on the manuscript. We acknowledge the Torrey Mesa Research Institute (San Diego) and the Salk Institute for Biological Studies (La Jolla) for providing insertion lines, and the Arabidopsis Biological Resource Center for providing clones. This work was supported by the National Science Foundation (IBN-0110667).

References

Ambrose, B. A., Lerner, D. R., Ciceri, P., Padilla, C. M., Yanofsky, M. F. and Schmidt, R. J. (2000). Molecular and genetic analyses of the *Silky1* gene reveal conservation in floral organ specification between eudicots and monocots. *Mol. Cell* **5**, 569-579.

Borden, K. L. B. (1998). RING fingers and B-boxes: zinc-binding protein-protein interaction domains. *Biochem. Cell Biol.* **76**, 351-358.

Bottomley, M. J., Collard, M. W., Huggenvik, J. I., Liu, Z., Gibson, T. J. and Sattler, M. (2001). The SAND domain structure defines a novel DNA-binding fold in transcriptional regulation. *Nat. Struct. Biol.* **8**, 626-633.

Boulikas, T. (1994). Putative nuclear localization signals (NLS) in protein transcription factors. *J. Cell Biochem.* **55**, 32-58.

Brand, U., Fletcher, J. C., Hobe, M., Meyerowitz, E. M. and Simon, R. (2000). Dependence of stem cell fate in *Arabidopsis* on a feedback loop regulated by *CLV3* activity. *Science* **289**, 617-619.

Bundock, P. and Hooykaas, P. (2002). Severe developmental defects, hypersensitivity to DNA-damaging agents, and lengthened telomeres in Arabidopsis MRE11 mutants. *Plant Cell* **14**, 2451-2462.

Burnett, E., Christensen, J. and Tattersall, P. (2001). A consensus DNA recognition motif for two KDWK transcription factors identifies flexible-length, CpG-methylation sensitive cognate binding sites in the majority of human promoters. *J. Mol. Biol.* **314**, 1029-1039.

Carles, C. C., Lertpiriyapong, K., Reville, K. and Fletcher, J. C. (2004). The *ULTRAPETALA1* gene functions early in Arabidopsis development to restrict shoot apical meristem activity, and acts through *WUSCHEL* to regulate floral meristem determinacy. *Genetics* **167**, 1893-1903.

Clark, S. E., Running, M. P. and Meyerowitz, E. M. (1993). *CLAVATA1*, a regulator of meristem and flower development in *Arabidopsis*. *Development* **119**, 397-418.

Clark, S. E., Running, M. P. and Meyerowitz, E. M. (1995). *CLAVATA3* is a specific regulator of shoot and floral meristem development affecting the same processes as *CLAVATA1*. *Development* **121**, 2057-2067.

Clark, S. E., Williams, R. W. and Meyerowitz, E. M. (1997). The CLAVATA1 gene encodes a putative receptor kinase that controls shoot and floral meristem size in *Arabidopsis*. *Cell* **89**, 575-585.

Clough, S. J. and Bent, A. F. (1998). Floral dip: a simplified method for Agrobacterium-mediated transformation of *Arabidopsis thaliana*. *Plant J.* **16**, 735-743.

Fabbro, M. and Henderson, B. R. (2003). Regulation of tumor suppressors by nuclear-cytoplasmic shuttling. *Exp. Cell Res.* **282**, 59-69.

Fletcher, J. C. (2001). The *ULTRAPETALA* gene controls shoot and floral meristem size in Arabidopsis. *Development* **128**, 1323-1333.

Fletcher, J. C., Brand, U., Running, M. P., Simon, R. and Meyerowitz, E. M. (1999). Signaling of cell fate decisions by *CLAVATA3* in *Arabidopsis* shoot meristems. *Science* **283**, 1911-1914.

Gallois, J.-L., Woodward, C., Reddy, G. V. and Sablowski, R. (2002). Combined SHOOT MERISTEMLESS and WUSCHEL trigger ectopic organogenesis in *Arabidopsis*. *Development* **129**, 3207-3217.

Gibson, T. J., Ramu, C., Gemund, C. and Aasland, R. (1998). The APECED polyglandular autoimmune syndrome protein, AIRE-1, contains the SAND domain and is probably a transcription factor. *Trends Biochem. Sci.* **23**, 242-244.

Gleave, A. P. (1992). A versitile binary vector system with a T-DNA organizational structure conducive to efficient integration of cloned DNA into the plant genome. *Plant Mol. Biol.* **20**, 1203-1207.

Grebenok, R. J., Peirson, E., Lambert, G. M., Gong, F.-C., Afonso, C. L., Haldeman-Cahill, R., Carrington, J. C. and Galbraith, D. W. (1997). Green florescent protein fusions for efficient characterization of nuclear targeting. *Plant J.* **11**, 573-586.

Gross, C. T. and McGinnis, W. (1996). DEAF-1, a novel protein that binds an essential region in a Deformed response element. *EMBO J.* **15**, 1961-1970.

Guyomarc'h, S., Vernoux, T., Traas, J., Zhou, D. X. and Delarue, M. (2004). *MGOUN3*, an Arabidopsis gene with TetratricoPeptide-Repeat-related motifs, regulates meristem cellular organization. *J. Exp. Bot.* **55**, 673-684.

Halonen, M., Kangas, H., Ruppell, T., Ilmarinen, T., Ollila, J., Kolmer, M., Vihinen, M., Palvimo, J., Saarela, J., Ulmanen, I. et al. (2004). APECED-causing mutations in AIRE reveal the functional domains of the protein. *Hum. Mutat.* **23**, 245-257.

Hicks, G. R. and Raikhel, N. V. (1995). Protein import into the nucleus: an integrated view. *Annu. Rev. Cell Dev. Biol.* **11**, 155-188.

Hulo, N., Sigrist, C. J. A., le Saux, V., Langendijk-Genevaux, P. S., Bordoli, L., Gattiker, A., de Castro, E., Bucher, P. and Bairoch, A. (2004). Recent improvements to the PROSITE database. *Nucleic Acids Res.* **32**, D134-D137.

Jeong, S., Trotochaud, A. E. and Clark, S. E. (1999). The *Arabidopsis CLAVATA2* gene encodes a receptor-like protein required for the stability of the *CLAVATA1* receptor-like kinase. *Plant Cell* **11**, 1925-1933.

Jimenez-Lara, A. M., Heine, M. J. and Gronemeyer, H. (2000). Cloning of a mouse glucocorticoid modulatory element binding protein, a new member of the KDWK family. *FEBS Lett.* **468**, 203-210.

Kaya, H., Shibahara, K., Taoka, K., Iwabuchi, M., Stillman, B. and Araki, T. (2001). *FASCIATA* genes for Chromatin Assembly Factor-1 in *Arabidopsis* maintain the cellular organization of apical meristems. *Cell* **104**, 131-142.

Kayes, J. M. and Clark, S. E. (1998). *CLAVATA2*, a regulator of meristem and organ development in *Arabidopsis*. *Development* **125**, 3843-3851.

Konieczny, A. and Ausubel, F. M. (1993). A procedure for mapping Arabidopsis mutations using co-dominant ecotype-specific PCR-based markers. *Plant J.* **4**, 403-410.

Laux, T., Mayer, K. F. X., Berger, J. and Jurgens, G. (1996). The *WUSCHEL* gene is required for shoot and floral meristem integrity in *Arabidopsis*. *Development* **122**, 87-96.

Lenhard, M. and Laux, T. (2003). Stem cell homeostasis in the *Arabidopsis* shoot meristem is regulated by intercellular movement of CLAVATA3 and its sequestration by CLAVATA1. *Development* **130**, 3163-3173.

Leyser, H. M. O. and Furner, I. J. (1992). Characterisation of three shoot apical meristem mutants of *Arabidopsis thaliana*. *Development* **116**, 397-403.

Long, J. A. and Barton, M. K. (1998). The development of apical embryonic pattern in *Arabidopsis*. *Development* **125**, 3027-3035.

Long, J. and Barton, M. K. (2000). Initiation of axillary and floral meristems in Arabidopsis. *Dev. Biol.* **218**, 341-353.

Long, J. A., Moan, E. I., Medford, J. I. and Barton, M. K. (1996). A

member of the KNOTTED class of homeodomain proteins encoded by the *STM* gene of *Arabidopsis*. *Nature* **379**, 66-69.
Mayer, K. F. X., Schoof, H., Haecker, A., Lenhard, M., Jurgens, G. and Laux, T. (1998). Role of *WUSCHEL* in regulating stem cell fate in the *Arabidopsis* shoot meristem. *Cell* **95**, 805-815.
McConnell, J. R. and Barton, M. K. (1998). Leaf polarity and meristem formation in *Arabidopsis*. *Development* **125**, 2935-2942.
McGuffin, L. J., Bryson, K. and Jones, D. T. (2000). The PSIPRED protein structure prediction server. *Bioinformatics* **16**, 404-405.
Merkle, T. (2001). Nuclear import and export of proteins in plants: a tool for the regulation of signalling. *Planta* **213**, 499-517.
Nair, R., Carter, P. and Rost, B. (2003). NLSdb: database of nuclear localization signals. *Nucleic Acids Res.* **31**, 397-399.
Nakai, K. and Kanehisa, M. (1992). A knowledge base for predicting protein localization sites in eukaryotic cells. *Genomics* **14**, 897-911.
Nielsen, H., Engelbrecht, J., Brunak, S. and von Heijne, G. (1997). Identification of prokaryotic and eukaryotic signal peptides and predictions of their cleavage sites. *Prot. Eng.* **10**, 1-6.
Peterson, P., Pitkänen, J., Sillanpaa, N. and Krohn, K. (2004). Autoimmune polyendocrinopathy candidiasis ectodermal dystrophy (APECED): a model disease to study molecular aspects of endocrine autoimmunity. *Clin. Exp. Immunol.* **135**, 348-357.
Pitkänen, J., Vähämurto, P., Krohn, K. and Peterson, P. (2001). Subcellular localization of the autoimmune regulator protein. characterization of nuclear targeting and transcriptional activation domain. *J. Biol. Chem.* **276**, 19597-19602.
Raikhel, N. V. (1992). Nuclear targeting in plants. *Plant Physiol.* **100**, 1627-1632.
Ramsey, C., Bukrinsky, A. and Peltonen, L. (2002). Systematic mutagenesis of the functional domains of AIRE reveals their role in intracellular targeting. *Hum Mol Genet.* **11**, 3299-3308.
Running, M. P., Fletcher, J. C. and Meyerowitz, E. M. (1998). The *WIGGUM* gene is required for proper regulation of floral meristem size in *Arabidopsis*. *Development* **125**, 2545-2553.
Running, M. P., Lavy, M., Sternberg, H., Galichet, A., Gruissem, W., Hake, S., Ori, N. and Yalovsky, S. (2004). Enlarged meristems and delayed growth in *plp* mutants result from lack of CaaX prenyltransferases. *Proc. Natl. Acad. Sci. USA* **101**, 7815-7820.
Sanford, J. C., Smith, F. D. and Russell, J. A. (1993). Optimizing the biolistic process for different biological applications. *Methods Enzymol.* **217**, 483-509.
Schoof, H., Lenhard, M., Haecker, A., Mayer, K. F. X., Jurgens, G. and Laux, T. (2000). The stem cell population of *Arabidopsis* shoot meristems is maintained by a regulatory loop between the *CLAVATA* and *WUSCHEL* genes. *Cell* **100**, 635-644.
Siddiqui, N. U., Stronghill, P. E., Dengler, R. E., Hasenkampf, C. A. and and Riggs, C. D. (2003). Mutations in Arabidopsis condensin genes disrupt embryogenesis, meristem organization and segregation of homologous chromosomes during meiosis. *Development* **130**, 3283-3295.
Sieburth, L. E. and Meyerowitz, E. M. (1997). Molecular dissection of the AGAMOUS control region shows that *cis* elements for spatial regulation are located intragenically. *Plant Cell* **9**, 355-365.
Sigrist, C. J. A., Cerutti, L., Hulo, N., Gattiker, A., Falquet, L., Pagni, M., Bairoch, A. and Bucher, P. (2002). PROSITE: a documented database using patterns and profiles as motif descriptors. *Brief Bioinform.* **3**, 265-274.
Steeves, T. A. and Sussex, I. M. (1989). *Patterns in Plant Development*. New York: Cambridge University Press.
Surdo, P. L., Bottomley, M. J., Sattler, M. and Scheffzek, K. (2003). Crystal structure and nuclear magnetic resonance analyses of the SAND domain from glucocorticoid modulatory element binding protein-1 reveals deoxyribonucleic acid and zinc binding regions. *Mol. Endocrinol.* **17**, 1283-1295.
Suzuki, T., Inagaki, S., Nakijima, S., Akashi, T., Ohto, M., Kobayashi, M., Seki, M., Shinozaki, K., Kato, T., Tabata, S. et al. (2004). A novel Arabidopsis gene *TONSOKU* is required for proper cell arrangement in root and shoot apical meristem. *Plant J.* **38**, 673-684.
Takeda, S., Hofmann, I., Probst, A. V., Angelis, K. J., Kaya, H., Araki, T., Mengiste, T., Scheid, O. M., Shibahara, K. et al. (2004). BRU1, a novel link between responses to DNA damage and epigenetic gene silencing in Arabidopsis. *Genes Dev.* **18**, 782-793.
Torok, M. and Etkin, L. D. (2000). Two B or not two B? Overview of the rapidly expanding B-box family of proteins. *Differentiation* **67**, 63-71.
Trotochaud, A. E., Hao, T., Wu, G., Yang, Z. and Clark, S. E. (1999). The CLAVATA1 receptor-like kinase requires CLAVATA3 for its assembly into a signaling complex that includes KAPP and a Rho-related protein. *Plant Cell* **11**, 393-405.
Ueda, M., Matsui, K., Ishiguro, S., Sano, R., Wada, T., Paponov, I., Palme, K. and Okada, K. (2004). The *HALTED ROOT* gene encoding the 26S proteasome subunit RPT2a is essential for the maintenance of Arabidopsis meristems. *Development* **131**, 2101-2111.
Ziegelbauer, J., Shan, B., Yager, D., Larabell, C., Hoffmann, B. and Tjian, R. (2001). Transcription factor MIZ-1 is regulated via microtubule association. *Mol. Cell* **8**, 339-349.
Ziegelhoffer, E. C., Medrano, L. J. and Meyerowitz, E. M. (2000). Cloning of the *Arabidopsis WIGGUM* gene identifies a role for farnesylation in meristem development. *Proc. Natl. Acad. Sci. USA* **97**, 7633-7638.